Available online at www.sciencedirect.com
ScienceDirect
Inorganica Chimica Acta 360 (2007) 3543–3552
Inorganica Chimica Acta
www.elsevier.com/locate/ica

Adducts of europium β-diketonates with nitrogen *p*,*p*′-disubstituted bipyridine and phenanthroline ligands: Synthesis, structural characterization, and luminescence studies

Channa R. De Silva [a], Jenine R. Maeyer [a], Ruiyao Wang [b], Gary S. Nichol [a], Zhiping Zheng [a,*]

[a] *Department of Chemistry, University of Arizona, Tucson, AZ 85721, USA*
[b] *Department of Chemistry, Queen's University, Kingston, Ontario, Canada K7L 3N6*

Received 26 November 2006; received in revised form 12 April 2007; accepted 17 April 2007
Available online 13 May 2007

Abstract

Europium complexes featuring fluorinated β-diketonate ligands [thenoyltrifluoroacetone (tta), 4,4,4-trifluoro-1-phenyl-1,3-butanedione (btfac), and 1,1,1,5,5,5-hexafluoro-2,4-pentanedionate (hfac)] and nitrogen *p*,*p*′-disubstituted bipyridine and phenanthroline ligands [4,4′-dimethoxy-2,2′-bipyridine (dmbipy) and 4,7-dimethyl-1,10-phenanthroline (dmphen)] were synthesized. Their structures were determined by single crystal X-ray diffraction. Octacoordinate complexes were obtained using trifluorinated tta and btfac, while nonacoordinated complexes were produced using hexafluorinated hfac. The differences in coordination number and bond lengths of these complexes are rationalized in terms of the electronic and steric features of the ligands. UV excitation of the complexes led to red luminescence characteristic of trivalent europium ion. The high overall quantum yields observed for the europium complexes bearing hfac and dmbipy or dmphen ligands are rationalized in terms of the relatively high ligand-to-metal energy transfer efficiencies.

Keywords: Europium complex; β-Diketonates; X-ray crystallography; Luminescence property

1. Introduction

Luminescent lanthanide complexes are an important class of materials. Their unique properties include long luminescence lifetimes, narrower emission, large stoke shift, high luminescence quantum efficiency, and decoupled functionalization of the supporting ligands from the metal-based luminescence [1]. Diverse applications, envisioned or realized, include their uses as emissive materials in organic light-emitting diodes [2], bio-immunoassays [3], and in sensory technology [4]. Not surprisingly, the synthesis and property studies of such materials remain an active area of lanthanide research.

However, f–f transitions are forbidden by the parity rule, and in many cases, also by the spin rule, leading to very small absorption cross-sections and low molar absorptivities [5]. As such, direct excitation of f electrons to the emissive state is difficult. Utilizing certain ligands as "antenna" to mediate energy transfer, the lanthanide ions can be sensitized effectively [6]. The commonly accepted mechanism for such sensitization entails light absorption by the ligands, populating the ligand triplet states via intersystem crossing, intramolecular energy transfer from the ligand triplet states to the emissive state(s) of the lanthanide center, and finally light emission characteristic of a specific lanthanide ion [7].

Lanthanide β-diketonates are the most extensively studied class of compounds in this particular area of lanthanide research, as stable and highly efficient luminescent complexes can be prepared by using these readily accessible

* Corresponding author. Tel.: +1 520 626 6495; fax: +1 520 621 8407.
E-mail address: zhiping@u.arizona.edu (Z. Zheng).

0020-1693/$ - see front matter © 2007 Elsevier B.V. All rights reserved.
doi:10.1016/j.ica.2007.04.049

ligands [8]. Among the many β-diketonate ligands studied, those that are equipped with fluorinated functional groups received particular attention because the presence of C–F bonds, as opposed to C–H, a higher-energy frequency oscillator, helps reduce nonradiative quenching of lanthanide luminescence [9]. Additional advantages of using fluorinated ligands include enhanced thermal stability and volatility of the complexes; both are of significance in practical applications of luminescent lanthanide materials [10].

As typically prepared by a reaction in aqueous solution using a mixture in 1:3 molar ratio of a lanthanide salt and a chosen β-diketonate ligand, a hydrate of the neutral complex of the general formula Ln(β-diketonate)$_3 \cdot (H_2O)_n$ is obtained [11]. The presence of the aqua ligands is due to the high coordination number requirement of the rather bulky lanthanide ions. For the synthesis of luminescent complexes, these coordinated water molecules need to be replaced by other type of Lewis base ligands that do not contain O–H bonds; similar to C–H and N–H bonds, dipole–dipole coupling with this high energy oscillator significantly quenches the luminescence. Accordingly, numerous adducts of lanthanide β-diketonates of the general formula Ln(β-diketonate)$_3 \cdot$ L are prepared, wherein L represents a neutral Lewis base ligand such as 2,2′-bipyridine [12] and 1,10-phenanthroline [13]. Other commonly used neutral ligands include triphenylphosphine oxide, diglyme, and various analogs or derivatives of these ligands [9b,14–17].

We have been interested in utilizing luminescent lanthanide complexes as the emissive materials in organic light-emitting devices [18]. A series of nonacoordinated adducts of europium β-diketonates with 2,4,6-tri(2-pyridyl)-1,3,5-triazine, a terdentate neutral ligand, have recently been reported, some of which display impressive luminescence quantum yields up to 70% [19–21]. As part of our continued efforts, we report here the synthesis, structural characterization, and photoluminescence properties of five new lanthanide complexes featuring fluorinated β-diketonates and nitrogen *p*,*p*′-disubstituted derivatives of 2,2′-bipyridine and 1,10-phenanthroline. The ligands utilized in the present study, benzoyltrifluoroacetone (Hbtfac), hexafluoroacetylacetone (Hhfac), and thenoyltrifluoroacetone (Htta), are among the most commonly used fluorinated β-diketonate ligands, while the bidentate neutral ligands, 4,4′-dimethoxy-2,2′-bipyridine (dmbipy) and 4,7-dimethyl-1,10-phenanthroline (dmphen), have been suggested for the development of luminescent lanthanide-containing liquid crystalline materials [16,22–24]. These ligands are collected and structurally shown in Fig. 1.

2. Experimental

2.1. General considerations

$EuCl_3 \cdot 6H_2O$, 1,1,1,5,5,5-hexafluoro-2,4-pentanedione, thenoyltrifluoroacetone, 4,4,4-trifluoro-1-phenyl-1,3-butanedione, 4-4′-dimethoxy-2,2′-bipyridine, 4,7-dimethyl-1,10-phenanthroline, and potassium *tert*-butoxide were purchased from Aldrich and used without further purification. The literature procedure for the synthesis of Eu(tta)$_3(H_2O)_2$ was followed as the first step of synthesis in this work [17]. Our recently reported procedure for the synthesis of Eu(hfac)$_3$-(tptz) was adopted for the ensuing substitution of aqua ligands for bidentate neutral ligands [20]. Elemental analysis (CHN) was performed by Numega Resonance Laboratory, San Diego, California.

2.1.1. Eu(tta)$_3$(dmbipy)

To an aqueous solution of KO′Bu (0.336 g, 3 mmol in 20 mL of H_2O) was added Htta (0.666 g, 3 mmol). The mixture was stirred for 10 min and the resulting clear solution was added to an aqueous solution of $EuCl_3 \cdot 6H_2O$ (0.366 g, 1 mmol in 10 mL of H_2O) to afford a white precipitate. This mixture was stirred under nitrogen at 60 °C for 30 min and then at room temperature for an additional 3 h. The precipitate was filtered off, washed with cold H_2O (2×100 mL), hexane (3 mL), and dried under vacuum for 12 h. Further purification of the product, Eu(tta)$_3(H_2O)_2$, was achieved by recrystallization from acetone:ethanol (v/v 1:1).

To a solution of Eu(tta)$_3(H_2O)_2$ (0.426 g, 0.5 mmol) in acetone (15 mL) was added dmbipy (0.108 g, 0.5 mmol in 15 mL of acetone). The resulting clear mixture was stirred at 60 °C for 30 min and then at room temperature for an additional 12 h. The mixture was filtered, and the filtrate was allowed to evaporate at room temperature to afford analytically pure product as a pale yellow solid (0.43 g,

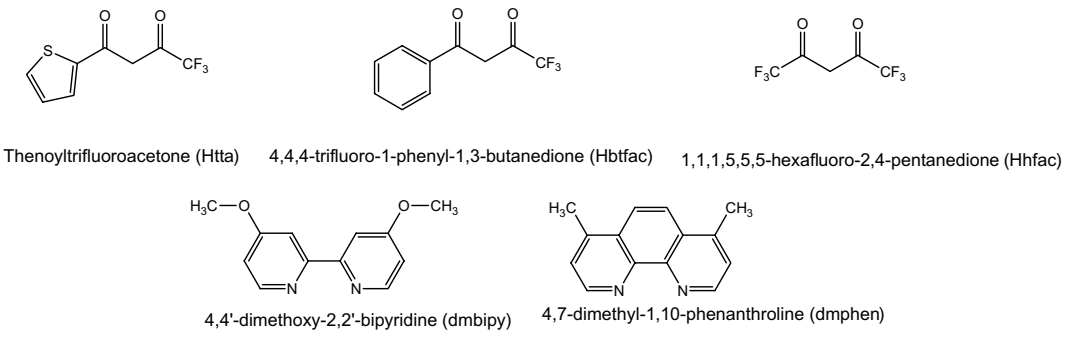

Fig. 1. Molecular structures of the ligands used in this work.

83%). *Anal.* Calc. for $C_{36}H_{24}N_2O_8F_9S_3Eu$: C, 41.91; H, 2.34; N, 2.72. Found: C, 41.74; H, 2.45; N, 2.86%.

2.1.2. Eu(btfac)$_3$(dmbipy) and Eu(hfac)$_3$(dmbipy)(H$_2$O)

These compounds were prepared by starting with Hbtfac (0.648 g, 3.00 mmol) and Hhfac (0.624 g, 3.00 mmol), respectively, using otherwise identical preparative and purification procedures to those for Eu(tta)$_3$(dmbipy). Eu(btfac)$_3$(dmbipy) was obtained as a white crystalline solid (0.44 g, 86%). *Anal.* Calc. for $C_{42}H_{30}N_2O_8F_9Eu \cdot H_2O$: C, 48.92; H, 3.12; N, 2.71. Found: C, 48.46; H, 2.97; N, 2.71%. Eu(hfac)$_3$(dmbipy)(H$_2$O) was also obtained as a white crystalline solid (0.29 g, 47%). *Anal.* Calc. for $C_{39}H_{29}N_4O_{11}F_{18}Eu \cdot 1.5CHCl_3$: C, 34.67; H, 2.19; N, 3.99. Found: C, 34.63; H, 2.00; N, 3.99%.

2.1.3. Eu(tta)$_3$(dmphen) and Eu(hfac)$_3$(dmphen)(EtOH)

By adopting otherwise identical preparative and purification procedures for Eu(tta)$_3$(dmbipy), the two complexes were synthesized by using dmphen (0.104 g, 0.5 mmol) in ethanol/dichloromethane (15 mL/15 mL) and appropriate β-diketonate ligands. Eu(tta)$_3$(dmphen) was obtained as a pale yellow crystalline solid (0.41 g, 80%). *Anal.* Calc. for $C_{38}H_{24}N_2O_6F_9S_3Eu \cdot H_2O$: C, 43.80; H, 2.52; N, 2.70. Found: C, 43.52; H, 2.67; N, 2.91%. Eu(hfac)$_3$(dmphen)(EtOH) was obtained as a white crystalline solid (0.30 g, 60%). *Anal.* Calc. for $C_{43}H_{29}N_4O_7F_{18}Eu \cdot 2H_2O$: C, 42.50; H, 2.93; N, 4.41. Found: C, 42.51; H, 2.44; N, 4.62%.

2.2. X-ray structure determinations

Single crystals suitable for X-ray crystallography were obtained by slow evaporation of the saturated solutions of the europium complexes in ethanol:acetone:diethyl ether (v/v/v 1:1:0.5) at room temperature.

A crystal was mounted on a glass fiber in a random orientation. Examination of the crystal was carried out on a Bruker SMART 1000 CCD detector X-ray diffractometer at 170(2) K and a power setting of 50 kV, 40 mA. Data were collected on the SMART1000 system using graphite monochromated Mo Kα radiation ($\lambda =$ 0.71073 Å). The frames were integrated using the Bruker SAINT software package's narrow frame algorithm [25], and empirical absorption and decay corrections were applied using the program SADABS [26]. The structures were solved using SHELXS in the Bruker SHELXTL (Version 5.0) software package [25]. Refinements were performed using SHELXL and illustrations were made using DIAMOND. Solution was achieved utilizing direct methods followed by Fourier synthesis. Hydrogen atoms were added at idealized positions, constrained to ride on the atom to which they are bonded and given thermal parameters equal to 1.2 or 1.5 times U_{iso} of that bonded atom. Details on data collection and structure refinements are given in Table 1.

Some of the CF_3 groups are disordered in Eu(btfac)$_3$(dmbipy), Eu(hfac)$_3$(dmbipy)(H$_2$O), Eu(tta)$_3$(dmphen), and Eu(hfac)$_3$(dmphen)(EtOH). Disordering of the ligand CF_3 and thienyl groups is common in the structural determination of lanthanide β-diketonates. However, they do not affect the final refinements of the title complexes.

2.3. Photophysical studies

Electronic absorption spectra were recorded using dichloromethane solutions on a Perkin–Elmer Lambda 10 spectrophotometer. Photoluminescence studies were carried out with a Fluorolog-3 fluorometer. The measured fluorescence in the visible range was excited by radiation from a Xe-Arc lamp and detected with a photo multiplier tube at an angle of 90° to the incident beam.

Photoluminescent quantum yields of the title complexes in dichloromethane were measured and calculated using cresyl violet perchlorate ($\Phi = 0.54$ in methanol) [27] or rhodamine 6G ($\Phi = 0.95$ in ethanol) [28] as the standards. Instrumental corrections and refractive indices of the solvents were taken into account in the calculations [29]. The relative quantum yields were calculated using the following established equation where Abs, A, and n denote the absorbance at the excitation wavelength, integrated area of the corrected emission spectrum, and refractive index of the solvent, respectively. Subscripts R and S refer to the reference and the sample, respectively [30]. The experimental uncertainty of the calculated quantum yields is about 10%.

$$\Phi_S = \Phi_R(\mathrm{Abs}_R/\mathrm{Abs}_S)(A_S/A_R)(n_S^2/n_R^2)$$

The luminescence lifetime measurements were performed by excitation of dichloromethane solutions using a Nd:YAG laser (Powerlite 8010, wavelength 354 nm). Emission from the solutions was collected at a right angle to the excitation beam and selected using a Spectral Products monochromator. The signal was monitored by a photomultiplier (Hamamatsu R928) coupled to a 500 MHz bandpass digital oscilloscope (Tektronix TDS 620B). The signals (at least 5000 points for each trace) from >500 flashes were collected and averaged. Luminescence lifetimes are averages of at least three independent determinations.

3. Results and discussion

3.1. Synthesis and structural characterization

The complex synthesis was carried out according to the reported procedures. Shown in Scheme 1 as a representative is the synthesis of the dmbipy adducts of three different europium β-diketonates. The molar ratio between Eu(III) and β-diketonate ligands was kept at 1:3 in order to minimize the formation of anionic tetrakis β-diketonate complexes [11,31]. The hydrated complex can be obtained in a relatively pure form by slow addition of the β-diketonate ligand/base mixture to the aqueous solution of the lanthanide salt. If necessary, the crude products can be further purified by recrystallization from an acetone/ethanol mixture.

Table 1
Crystal data and structure refinement for $Eu(tta)_3(dmbipy)$, $Eu(btfac)_3(dmbipy)$, $Eu(hfac)_3(dmbipy)(H_2O)$, $Eu(tta)_3(dmphen)$, and $Eu(hfac)_3(dmphen)(EtOH)$

	$Eu(tta)_3(dmbipy)$	$Eu(btfac)_3(dmbipy)$	$Eu(hfac)_3(dmbipy)(H_2O)$	$Eu(tta)_3(dmphen)$	$Eu(hfac)_3(dmphen)(EtOH)$
Empirical formula	$C_{72}H_{48}Eu_2F_{18}N_4O_{16}S_6$	$C_{42}H_{30}EuF_9N_2O_8$	$C_{33}H_{23}EuF_{18}N_3O_{10}$	$C_{77}H_{56}Cl_2Eu_2F_{18}N_4O_{12}S_6$	$C_{45}H_{33}EuF_{18}N_4O_7$
Formula weight (g mol^{-1})	2063.42	1013.64	1115.5	2138.44	1235.71
Temperature (K)	180(2)	170(2)	170(2)	170(2)	180(2)
Wavelength (Å)	0.71073	0.71073	0.71073	0.71073	0.71073
Crystal system	orthorhombic	orthorhombic	monoclinic	monoclinic	monoclinic
Space group	*Pbca*	*Pbca*	*P*2(1)/*n*	*P*2(1)/*n*	*P*2(1)/*n*
Unit cell dimensions					
a (Å)	20.872(3)	20.908(8)	10.4247(12)	18.6012(11)	12.3239(14)
b (Å)	16.879(2)	17.001(7)	25.171(3)	20.2640(12)	27.050(3)
c (Å)	22.041(3)	22.754(9)	15.4695(17)	21.7675(13)	14.6778(16)
α (°)	90	90	90	90	90
β (°)	90	90	97.596(2)	92.9450(10)	92.820(2)
γ (°)	90	90	90	90	90
V (Å^3)	7764.8(17)	8088(5)	4023.6(8)	8194.1(8)	4887.1(9)
Z	4	8	4	4	4
D_{calc} (mg/m^3)	1.765	1.665	1.841	1.733	1.679
Absorption coefficient (mm^{-1})	1.874	1.648	1.7	1.839	1.405
F(000)	4080	4032	2188	4240	2448
Crystal size (mm^3)	$0.40 \times 0.30 \times 0.15$	$0.29 \times 0.25 \times 0.20$	$0.37 \times 0.26 \times 0.26$	$0.27 \times 0.26 \times 0.20$	$0.35 \times 0.32 \times 0.25$
θ Range for utilized data (°)	1.85–25.00	1.80–25.00	1.56–27.04	2.2–25.0	2.05–25.00
Limiting indices	$-24 \leqslant h \leqslant 22$, $-18 \leqslant k \leqslant 20$, $-25 \leqslant l \leqslant 26$	$-24 \leqslant h \leqslant 24$, $-20 \leqslant k \leqslant 20$, $-27 \leqslant l \leqslant 27$	$-13 \leqslant h \leqslant 13$, $-32 \leqslant k \leqslant 32$, $-19 \leqslant l \leqslant 19$	$-23 \leqslant h \leqslant 23$, $-25 \leqslant k \leqslant 25$, $-27 \leqslant l \leqslant 27$	$-14 \leqslant h \leqslant 14$, $-31 \leqslant k \leqslant 32$, $-17 \leqslant l \leqslant 16$
Reflections utilized	43214	75444	45493	89842	28471
Independent reflections [R_{int}]	6820 [0.1271]	7114 [0.1100]	8793 [0.0387]	17047 [0.0491]	8612 [0.0241]
Completeness to θ	100.0% ($\theta = 25.00°$)	100.0% ($\theta = 23.27°$)	99.7% ($\theta = 27.04°$)	99.9% ($\theta = 26.50°$)	99.9% ($\theta = 25.00°$)
Absorption correction	empirical (Bruker SADABS)	semi-empirical from equivalents	semi-empirical from equivalents	semi-empirical from equivalents	empirical (Bruker SADABS)
Maximum and minimum transmission	1.0 and 0.4754	0.7308 and 0.6464	0.6691 and 0.5757	0.7088 and 0.6347	1.0000 and 0.8013
Refinement method	full-matrix least-squares on F^2	full-matrix least-squares on F^2	full-matrix least-squares on F^2	full-matrix least-squares on F^2	full-matrix least-squares on F^2
Data/restraints/parameters	6820/0/517	7114/84/579	8793/678/641	17047/24/1126	8612/29 /843
Goodness-of-fit on F^2	1.000	1.161	1.094	1.057	1.000
Final *R* indices [$I > 2\sigma(I)$]	$R_1 = 0.0710$, $wR_2 = 0.1612$	$R_1 = 0.0599$, $wR_2 = 0.856$	$R_1 = 0.0372$, $wR_2 = 0.0756$	$R_1 = 0.0470$, $wR_2 = 0.1099$	$R_1 = 0.0305$, $wR_2 = 0.0787$
R indices (all data)	$R_1 = 0.1283$, $wR_2 = 0.1840$	$R_1 = 0.0898$, $wR_2 = 0.0931$	$R_1 = 0.0484$, $wR_2 = 0.0794$	$R_1 = 0.0636$, $wR_2 = 0.1171$	$R_1 = 0.0395$, $wR_2 = 0.0819$
Largest difference in peak and hole (e Å^{-3})	2.295 and −1.800	0.91 and −0.62	1.079 and −0.518	1.63 and −1.13	0.800 and −0.468

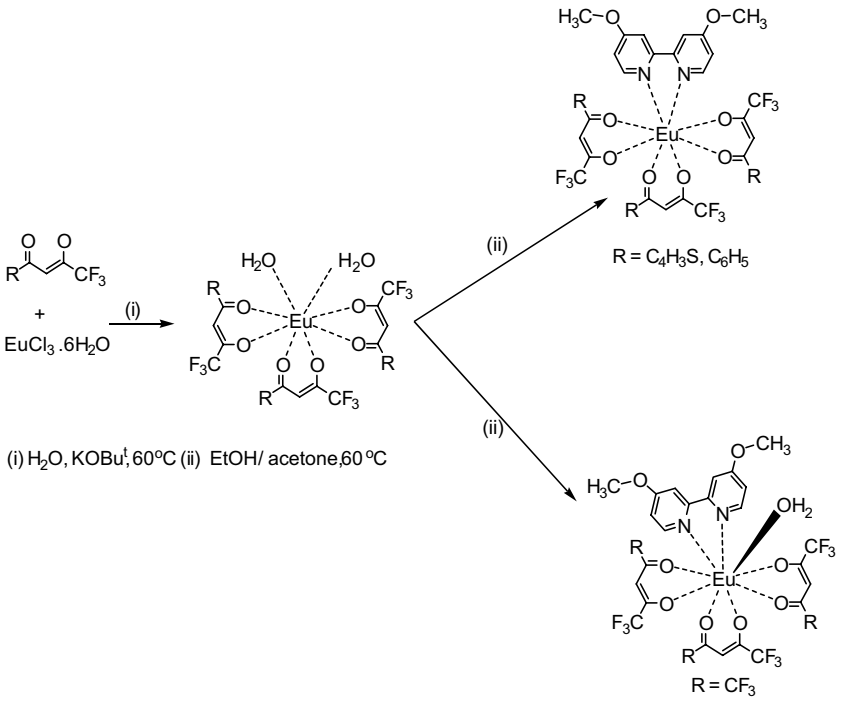

Scheme 1. Synthesis of Eu(β-diketonate)$_3$(dmbipy) complexes.

The aqua ligands were then replaced by reacting the hydrates with 4,4′-dimethoxy-2,2′-bipyridine (dmbipy) or 4,7-dimethyl-1,10-phenanthroline (dmphen). The substitution of the neutral ligands with electron-donating methoxy and methyl groups putatively enhances the coordinating ability over their unsubstituted parents, as discussed by Bellusci et al. [16].

The molecular structures of the five complexes were established by single-crystal X-ray diffraction, and are shown in Figs. 2–6. Selected metric values of bond distances and angles are summarized in Table 2.

Eu–O bond distances of Eu(tta)$_3$(dmbipy) [2.355(7)–2.393(6) Å; average 2.364 Å], Eu(btfac)$_3$(dmbipy) [2.367(4)–2.390(4) Å; average 2.375 Å], Eu(hfac)$_3$(dmbipy)(H$_2$O) [2.379(2)–2.510(2) Å; average 2.430 Å], Eu(tta)$_3$(dmphen) [2.329(3)–2.412(3) Å; average 2.366 Å], and Eu(hfac)$_3$-(dmphen)(EtOH) [2.386(2)–2.494(2) Å; average 2.435 Å] are within the normal bond distance range for europium β-diketonates. However, a more careful analysis of the metric data reveals a subtle, yet noticeable difference in the Eu–O distance amongst the five complexes. The Eu–O bonds are longer (2.430 and 2.435 Å) in the hfac com-

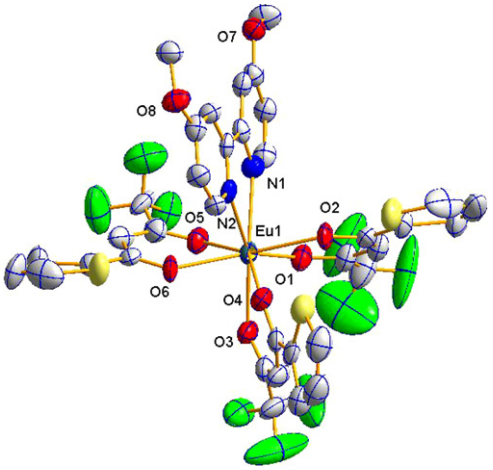

Fig. 2. An ORTEP view of the crystal structure of Eu(tta)$_3$(dmbipy) with partial atomic labeling. Thermal ellipsoids are drawn at the 50% probability level.

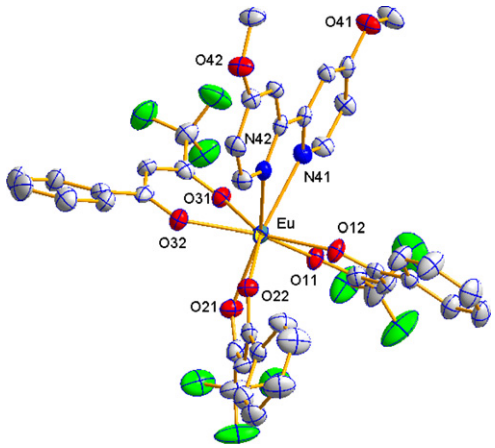

Fig. 3. An ORTEP view of the crystal structure of Eu(btfac)$_3$(dmbipy) with partial atomic labeling. Thermal ellipsoids are drawn at the 50% probability level.

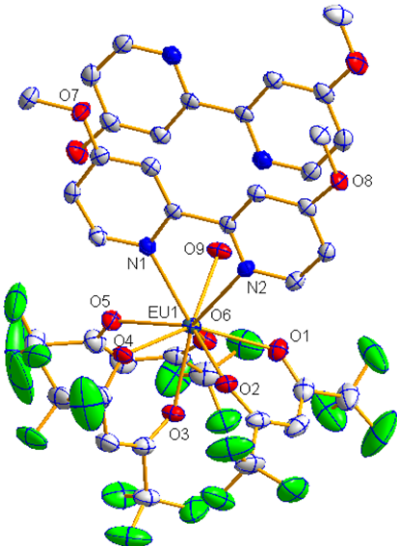

Fig. 4. An ORTEP view of the crystal structure of $Eu(hfac)_3(dmbipy)\cdot(H_2O)\cdot dmbipy$ with partial atomic labeling. Thermal ellipsoids are drawn at the 50% probability level.

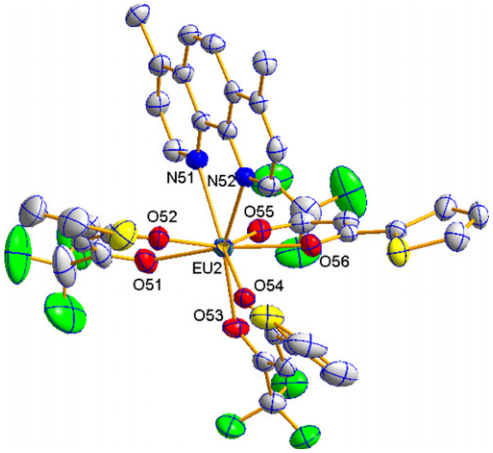

Fig. 5. An ORTEP view of the crystal structure of $Eu(tta)_3(dmphen)$ with partial atomic labeling. Thermal ellipsoids are drawn at the 50% probability level.

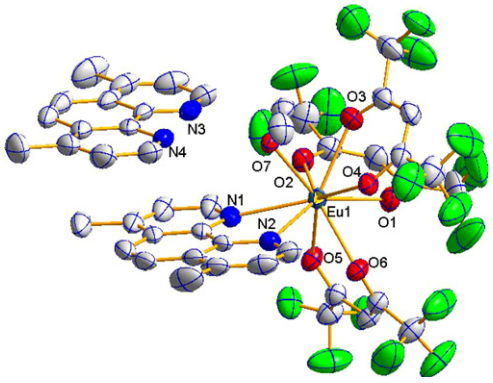

Fig. 6. Molecular Structure of $Eu(hfac)_3(dmphen)(EtOH)\cdot dmphen$. (Displacement ellipsoids for non-Hatoms are shown at the 50% probability level and H atoms are represented by circles of arbitrary size.)

Table 2
Selected bond distances (Å) and angles (°) of $Eu(tta)_3(dmbipy)$, $Eu(btfac)_3(dmbipy)$, $Eu(hfac)_3(dmbipy)(H_2O)$, $Eu(tta)_3(dmphen)$, and $Eu(hfac)_3(dmphen)(EtOH)$

$Eu(tta)_3(dmbipy)$	
Eu(1)–O(1)	2.359(7)
Eu(1)–O(2)	2.360(6)
Eu(1)–O(3)	2.355(7)
Eu(1)–O(4)	2.358(7)
Eu(1)–O(5)	2.357(6)
Eu(1)–O(6)	2.393(6)
Eu(1)–N(1)	2.551(8)
Eu(1)–N(2)	2.544(7)
O(1)–Eu(1)–O(2)	71.4(2)
O(2)–Eu(1)–O(3)	107.4(2)
O(3)–Eu(1)–O(4)	72.4(2)
O(4)–Eu(1)–O(5)	144.2(2)
O(5)–Eu(1)–O(6)	72.1(2)
O(1)–Eu(1)–N(1)	79.3(2)
O(6)–Eu(1)–N(2)	73.0(2)
N(1)–Eu(1)–N(2)	62.8(2)
$Eu(btfac)_3(dmbipy)$	
Eu–O(11)	2.367(4)
Eu–O(12)	2.364(4)
Eu–O(21)	2.370(4)
Eu–O(22)	2.384(4)
Eu–O(31)	2.373(4)
Eu–O(32)	2.390(4)
Eu–N(41)	2.566(5)
Eu–N(42)	2.567(4)
O(11)–Eu–O(12)	71.51(13)
O(12)–Eu–O(21)	106.80(14)
O(21)–Eu–O(22)	71.67(13)
O(22)–Eu–O(31)	142.76(13)
O(31)–Eu–O(32)	71.06(13)
O(11)–Eu–N(41)	78.46(14)
O(32)–Eu–N(42)	75.00(13)
N(41)–Eu–N(42)	62.58(14)
$Eu(hfac)_3(dmbipy)(H_2O)$	
Eu(1)–O(1)	2.379(2)
Eu(1)–O(2)	2.463(2)
Eu(1)–O(3)	2.406(2)
Eu(1)–O(4)	2.409(2)
Eu(1)–O(5)	2.417(2)
Eu(1)–O(6)	2.510(2)
Eu(1)–O(9)	2.445(2)
Eu(1)–N(1)	2.590(3)
Eu(1)–N(2)	2.606(3)
O(1)–Eu(1)–O(2)	69.56(8)
O(2)–Eu(1)–O(3)	70.21(8)
O(3)–Eu(1)–O(4)	72.43(8)
O(4)–Eu(1)–O(5)	71.36(8)
O(5)–Eu(1)–O(6)	68.11(8)
O(1)–Eu(1)–N(1)	36.14(8)
O(6)–Eu(1)–N(2)	128.59(8)
N(1)–Eu(1)–N(2)	62.18(8)
$Eu(tta)_3(dmphen)$	
Eu(1)–O(1)	2.373(3)
Eu(1)–O(2)	2.347(3)
Eu(1)–O(3)	2.373(3)
Eu(1)–O(4)	2.365(3)
Eu(1)–O(5)	2.329(3)

Table 2 (*continued*)

Eu(1)–O(6)	2.412(3)
Eu(1)–N(1)	2.594(4)
Eu(1)–N(2)	2.568(4)
O(1)–Eu(1)–O(2)	71.82(12)
O(2)–Eu(1)–O(3)	149.22(12)
O(3)–Eu(1)–O(4)	70.99(11)
O(4)–Eu(1)–O(5)	85.15(12)
O(5)–Eu(1)–O(6)	72.61(12)
O(1)–Eu(1)–N(1)	76.34(12)
O(6)–Eu(1)–N(2)	83.75(12)
N(1)–Eu(1)–N(2)	62.89(12)
Eu(hfac)$_3$(dmphen)(EtOH)	
Eu(1)–O(1)	2.398(3)
Eu(1)–O(2)	2.414(2)
Eu(1)–O(3)	2.494(2)
Eu(1)–O(4)	2.386(2)
Eu(1)–O(5)	2.479(2)
Eu(1)–O(6)	2.440(2)
Eu(1)–O(7)	2.456(2)
Eu(1)–N(1)	2.599(3)
Eu(1)–N(2)	2.590(3)
O(1)–Eu(1)–O(2)	73.91(8)
O(2)–Eu(1)–O(3)	66.92(8)
O(3)–Eu(1)–O(4)	68.83(8)
O(4)–Eu(1)–O(5)	134.86(7)
O(5)–Eu(1)–O(6)	68.15(7)
O(1)–Eu(1)–N(1)	137.06(9)
O(6)–Eu(1)–N(2)	70.53(8)
N(2)–Eu(1)–N(1)	63.02(9)

plexes than in the tta (2.364 and 2.366 Å) and btfac (2.375 Å) complexes.

Clearly, the metal coordination is influenced by the nature of the β-diketonate ligand, which can be rationalized by considering the enhanced electron-withdrawing power of the hexafluorinated hfac ligand versus the trifluorinated tta and btfac ligands; coordinating ability of the O atom in the former is weaker due to the presence of an additional electron-withdrawing CF_3 group in the former. The consequence is twofold: First, as bonding interactions of lanthanide compounds are primarily ionic, weaker interactions lead to longer Eu–O bonds, as observed. Second, a larger ligand-metal separation (the longer Eu–O bonds) releases more of the steric congestion around the lanthanide ion when compared with the complexes with tta or btfac, making facile the accommodation of the coordination-saturating neutral ligand(s), and possibly, a larger number of such ligands, thus resulting in a different metal coordination. This second anticipated consequence is clearly supported by the structures of the two hfac complexes in comparison with the other three (two with tta and one with btfac ligand). Specifically, complexes of the hexafluorinated hfac ligand feature a *nonacoordinate* metal center whose coordination polyhedron can be viewed as a distorted square antiprism monocapped by a coordinated water [in Eu(hfac)$_3$(dmbipy)(H_2O)] or ethanol [in Eu(hfac)$_3$(dmphen)(EtOH)]. Corroborating nonacoordinate complexes with the same β-diketonate ligand, Sm(hfac)$_3$(bipy)(H_2O) [32] and Eu(hfac)$_3$(bipy)(H_2O) [33], have recently appeared in the literature. In comparison, the use of the trifluorinated tta and btfac ligands affords *octacoordinate* complexes whose coordination polyhedra may be best described as distorted square antiprism.

Note that the dependence of lanthanide coordination on the size of the metal ion has previously been demonstrated by using adducts of lanthanide complexes of hfac with bipyridine and phenanthroline [32]. With a lighter and bulkier lanthanide ion such as La(III), inclusion of two bipy or phen ligands to achieve a coordination number of 10 is possible while a heavier and smaller metal ion such as Er(III) can only accommodate one such neutral ligand to produce an octacoordinate complex [32,34]. With an intermediate lanthanide ion such as Sm(III) or Eu(III), nonacoordinate complexes, Sm(hfac)$_3$(bipy)(H_2O) and Eu(hfac)$_3$(bipy)(H_2O), are obtained. For the same β-diketonate ligand, the two nonacoordinate complexes reported herein offer additional evidence to support the gradual transition of the coordination behavior across the lanthanide series.

The Eu–N bond length is normal, and the difference amongst the five complexes is insignificant. Although one may expect a shorter Eu–N bond in the hfac complexes due to the higher metal Lewis acidity, such effects may be offset by the increasing steric hindrance expected from a shortened Eu–N bond, especially when an additional neutral ligand is present. Interestingly, a molecule of non-coordinating dmbipy or dmphen is found in the solid state, engaging in π–π interactions with the coordinated neutral ligand. The aromatic centroid–centroid separation is 3.301–3.429 Å in Eu(hfac)$_3$(dmbipy)(H_2O) and 3.459–3.606 Å in Eu(hfac)$_3$(dmphen)(EtOH). Similar π–π interactions have also been observed in Sm(hfac)$_3$(bipy)(H_2O) and Eu(hfac)$_3$(bipy)(H_2O) [32,33]. The prevalent π–π interactions observed in complexes with the less basic hfac ligand (and hence more acidic metal ion) invite further investigation. It is reasonable to view the situation as one similar to the co-crystallization of hexafluorobenzene and benzene; the metal-bound and thus more electron-deficient aromatic ligand to the free ligand is as hexafluorobenzene to benzene. These observations further support the dominating influence of ligands on metal coordination behavior in lanthanide β-diketonates.

Aromatic-aromatic interactions have also been observed in Eu(tta)$_3$(dmphen), but between coordinated dmphen ligands (Fig. 7a). The closest distance between the two dmphen ligands is 3.9585 Å. In addition, the solid state structure of this complex shows two slightly different orientations of the tta and dmphen ligands with respect to the Eu(III) center. The two unique coordination geometries differ by subtle changes in the coordination environment and by slight conformational differences of the ligands caused by free rotation about some of the single bonds. In both complexes the phenanthroline ligand is essentially planar, and overlaying the mean planes shows relative positional difference of the remaining ligands (Fig. 7b). A similar behavior was reported for adducts of a series of

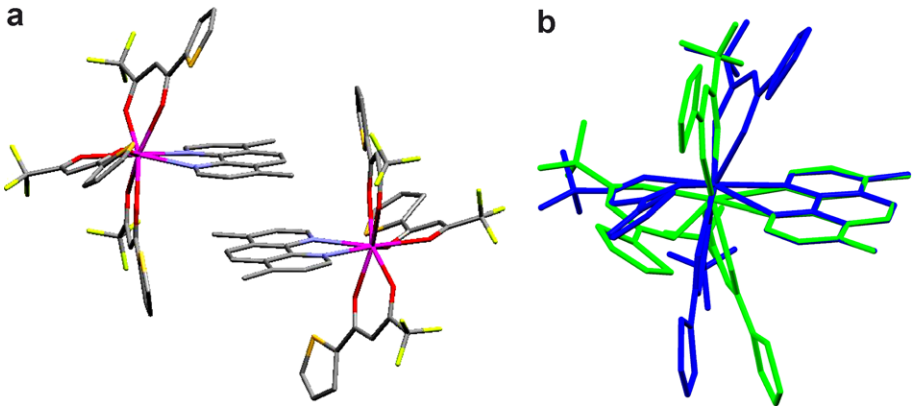

Fig. 7. (a) Highlighted aromatic stacking interactions between the two unique phenanthrolineligands in $Eu(tta)_3(dmphen)$. (b) An overlay (rms deviation = 0.0338 Å) of the two least-squares planes fitted through the phenanthroline ligands, showing the differences in coordination environment of the two europium centers, and the conformational differences of the remaining ligands in $Eu(tta)_3(dmphen)$.

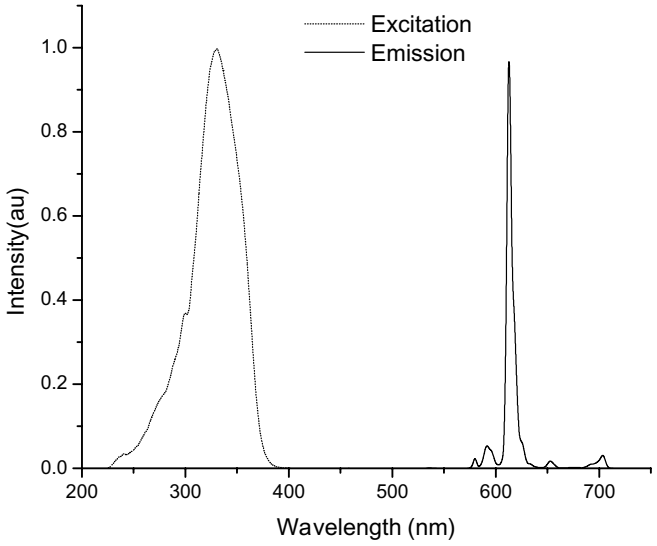

Fig. 8. The excitation (---) and emission (—) spectra of $Eu(btfac)_3(dmbipy)$ in CH_2Cl_2.

lanthanide β-diketonates with 2,9-dimethyl-1,10-phenanthroline [35].

3.2. Electronic spectroscopic and photoluminescence studies

Upon UV excitation all the complexes exhibit vivid red emission in both solid state and solution. The electronic excitation and photoluminescence spectra of $Eu(btfac)_3(dmbipy)$, representative of all the complexes reported herein, are shown in Fig. 8. Those for the other complexes are deposited as Supporting Materials.

The five narrow emission peaks can be assigned to $^5D_0 \rightarrow {}^7F_n$ ($n = 0$–4) transitions, of which the emission at 613 nm originated from $^5D_0 \rightarrow {}^7F_2$ electronic dipole transition is the strongest. Intensities of the strongest emissions of $Eu(tta)_3(dmbipy)$, $Eu(btfac)_3(dmbipy)$, $Eu(hfac)_3(dmbipy)(H_2O)$, $Eu(tta)_3(dmphen)$, and $Eu(hfac)_3(dmphen)(EtOH)$ are at maximum when the complexes are excited at 345, 331, 300, 343, and 306 nm, respectively. These excitation wavelengths are close to the absorption maxima of the corresponding β-diketonate ligands, suggesting that the sensitization of the emissive metal center is by energy transfer mediated by these ligands, consistent with the well-established mechanism of ligand-sensitized luminescence [6].

The overall quantum yield (Φ_{tot}) of a lanthanide complex does not provide information on the independent efficiency of ligand sensitization (η_{sens}) or that of lanthanide-centered luminescence (Φ_{Ln}). The overall quantum yield of ligand-sensitized lanthanide emission, determined experimentally, is the product of the ligand sensitization efficiency and the intrinsic quantum yield of the lanthanide luminescence according to [36].

$$\Phi_{tot} = \eta_{sens} \cdot \Phi_{Ln} \quad (1)$$

The intrinsic quantum yield of the lanthanide luminescence step (Φ_{Ln}) can be evaluated on the basis of observed luminescence lifetime (τ_{obs}) and pure radiative lifetime (τ_R) of the Eu(III) $^5D_0 \rightarrow {}^7F_n$ transitions by using [37].

$$\Phi_{Ln} = \tau_{obs}/\tau_R \quad (2)$$

$$1/\tau_R = A_{MD} \cdot n^3 \cdot (I_{tot}/I_{MD}) \quad (3)$$

where A_{MD} is the spontaneous emission probability for the $^5D_0 \rightarrow {}^7F_1$ magnetic dipole transition of Eu(III) ($A_{MD} = 14.65\ s^{-1}$), n the refractive index of the solvent, and (I_{tot}/I_{MD}) the ratio of the total area of the corrected Eu(III) emission spectrum to the area of the $^5D_0 \rightarrow {}^7F_1$ transition.

Table 3
Radiative lifetime (τ_R), observed luminescence lifetime (τ_{obs}), intrinsic quantum yield of the lanthanide luminescence (Φ_{Ln}), overall quantum yield (Φ_{tot}), and sensitization efficiency (η_{sens}) for Eu(III) complexes

Complex	τ_R (ms)	τ_{obs} (ms)	Φ_{Ln}	Φ_{tot}	η_{sens}
$Eu(tta)_3dmbipy$	1.51	0.67	0.45	0.23	0.52
$Eu(btfac)_3dmbipy$	1.53	0.75	0.49	0.18	0.37
$Eu(hfac)_3dmbipy(H_2O)$	1.62	0.33	0.21	0.48	2.35
$Eu(tta)_3dmphen$	1.54	0.69	0.45	0.34	0.76
$Eu(hfac)_3(dmphen)(EtOH)$	3.43	0.65	0.19	0.39	2.03

Radiative lifetimes (τ_R), intrinsic quantum yields of the lanthanide luminescence step (Φ_{Ln}), and sensitization efficiencies (η_{sens}) of the five Eu(III) complexes are calculated using Eqs. (1)–(3). These parameters along with the experimentally determined luminescence lifetimes (τ_{obs}) and overall quantum yields (Φ_{tot}) are summarized in Table 3.

The overall photoluminescence quantum yields (Φ_{tot}) of $Eu(tta)_3(dmbipy)$, $Eu(btfac)_3(dmbipy)$, $Eu(hfac)_3(dmbipy)(H_2O)$, $Eu(tta)_3(dmphen)$, and $Eu(hfac)_3(dmphen)(EtOH)$ were found to be 0.23, 0.18, 0.48, 0.34, and 0.39, respectively. Clearly the hfac ligand-bearing complexes display higher quantum yields than the other complexes.

Intrinsic quantum yields of $Eu(tta)_3dmbipy$, $Eu(btfac)_3dmbipy$, and $Eu(tta)_3dmphen$ are similar to one another due to their comparable coordination environments. These values are larger than those calculated for $Eu(hfac)_3dmbipy(H_2O)$ and $Eu(hfac)_3(dmphen)(EtOH)$. The luminescence lifetime (τ_{obs}) observed for $Eu(hfac)_3dmbipy(H_2O)$ is the shortest among the five complexes. It is understandable that the presence of the O–H oscillators in the close proximity of Eu(III) center effectively quenches the luminescence via vibrational relaxations [38]. As such, $Eu(hfac)_3dmbipy(H_2O)$ exhibits a relatively low intrinsic quantum yield value (Φ_{Ln}). A similar behavior was observed for $Eu(hfac)_3(dmphen)(EtOH)$. Thus, the observed higher overall quantum yields (Φ_{tot}) of $Eu(hfac)_3dmbipy(H_2O)$ and $Eu(hfac)_3(dmphen)(EtOH)$ must be due to the high efficiencies of ligand-to-metal energy transfer processes prior to lanthanide-centered luminescence, indicated by the sensitization efficiencies summarized in Table 3. The relatively high overall quantum yields suggest the potential applications of these complexes in electroluminescent devices. Our studies along this more technological line of research will be reported elsewhere.

4. Conclusions

Several new europium complexes with fluorinated β-diketonate ligands and nitrogen *p*,*p*′-disubstituted bipyridine and phenanthroline ligands were synthesized and their structures established by single-crystal X-ray diffraction. It has been shown that the lanthanide coordination behavior is significantly influenced by the β-diketonate ligands utilized, and to a much less extent, by the neutral ligands. The disparity of bond distance and coordination number can be rationalized in terms of the electronic and steric properties of the ligands. This work not only provides some luminescent lanthanide complexes, it also offers some much needed supporting evidence for drawing the conclusions elaborated above, that is, subtle but significant change in the coordination behavior can be achieved by judiciously chosen ligands. Photoluminescence studies show that excitation of the complexes is ligand based, and that the emission is characteristic of trivalent europium ion. The differences in overall quantum yields of the title complexes were evaluated in terms of their intrinsic quantum yields and the efficiencies of ligand sensitization.

Acknowledgements

This work was supported by NSF CAREER Grant No. CHE-0238790. Acknowledgment is also made to the Donors of The Petroleum Research Fund, administered by the American Chemical Society, for partial support of this research. The authors greatly appreciate the lifetime measurements by Professor S. Petoud and Mr. J. Zhang of University of Pittsburg. We thank Professor K. Miranda for the use of fluorometers. The CCD-based X-ray diffractometer was purchased through an NSF Grant (CHE-96103474, USA).

Appendix A. Supplementary material

CCDC Nos. 618404, 618405, 618406, 618407 and 618408 contain the supplementary crystallographic data for $Eu(tta)_3(dmbipy)$, $Eu(btfac)_3(dmbipy)$, $Eu(hfac)_3(dmbipy)(H_2O)$, $Eu(tta)_3(dmphen)$ and $Eu(hfac)_3(dmphen)(EtOH)$. These data can be obtained free of charge via http://www.ccdc.cam.ac.uk/conts/retrieving.html, or from the Cambridge Crystallographic Data Centre, 12 Union Road, Cambridge CB2 1EZ, UK; fax: (+44) 1223-336-033; or e-mail: deposit@ccdc.cam.ac.uk. Supplementary data associated with this article can be found, in the online version, at doi:10.1016/j.ica.2007.04.049.

References

[1] (a) I. Hemmila, V. Laitala, J. Fluoresc. 15 (2005) 529;
(b) H. Maas, A. Currao, C. Gion, Angew. Chem. Int. Ed. 41 (2002) 2495;
(c) C.H. Huang, F.Y. Li, W. Huang, Introduction to Organic Light-Emitting Materials and Devices, Fudan Press, Shanghai, China, 2005.
[2] (a) J. Kido, Y. Okamoto, Chem. Rev. 102 (2002) 2357;
(b) H. You, J. Fang, Y. Xuan, D. Ma, Mater. Sci. Eng. B131 (2006) 252.
[3] (a) F.S. Richardson, Chem. Rev. 82 (1982) 541;
(b) J. Yuan, G. Wang, J. Fluoresc. 15 (2005) 559.
[4] (a) J.G. Bunzli, Acc. Chem. Res. 39 (2006) 53;
(b) J.P. Leonard, T. Gunnlaugsson, J. Fluoresc. 15 (2005) 585.
[5] C. Görller-Walrand, in: K. Binnemans, K.A. Gschneidner Jr., L. Eyring (Eds.), Spectral Intensities of f–f Transitions in Handbook on the Physics and Chemistry of Rare Earths, vol. 25, North-Holland, Amsterdam, 1998.
[6] (a) S.I. Weissman, J. Chem. Phys. 10 (1942) 214;
(b) E.B. van der Tol, H.J. van Ramesdonk, J.W. Verhoeven, F.J. Steemers, E.G. Kerver, W. Verboom, D.N. Reinhoudt, Chem. Eur. J. 4 (1998) 2315;
(c) A.P. Bassett, S.W. Magennis, P.B. Glover, D.J. Lewis, N. Spencer, S. Parsons, R.M. Williams, L. De Cola, Z. Pikramenou, J. Am. Chem. Soc. 126 (2004) 9413.
[7] (a) G.A. Crosby, R.E. Whan, J.J. Freeman, J. Phys. Chem. 66 (1962) 2493;
(b) R.E. Whan, G.A. Crosby, J. Mol. Spectrosc. 8 (1962) 315;
(c) F.J. Steemers, W. Verboom, D.N. Reinhoudt, E.B. van der Tol, J.W. Verhoeven, J. Am. Chem. Soc. 117 (1995) 9408.
[8] K. Binnemans, Rare-earth beta-diketonates, in: K.A. Gschneidner Jr., J.-C.G. Bünzli, V.K. Pecharsky (Eds.), Handbook on the Physics and Chemistry of Rare Earths, vol. 35, Elsevier, 2005.
[9] (a) Y. Hasegawa, M. Yamamuro, Y. Wada, N. Kanehisha, Y. Kai, S. Yanagida, J. Phys. Chem. A 107 (2003) 1697;

(b) Y. Hasegawa, H. Kawai, K. Nakamura, N. Yasuda, Y. Wada, S. Yanagida, J. Alloys Compd. 408 (2006) 669.
[10] (a) R.E. Sievers, J.E. Sadlowski, Science 201 (1978) 217;
(b) J. Yu, L. Zhou, H. Zhang, Y. Zheng, H. Li, R. Deng, Z. Peng, Z. Li, Inorg. Chem. 44 (2005) 1611.
[11] L.R. Melby, N.J. Rose, E. Abramson, J.C. Caris, J. Am. Chem. Soc. 86 (1964) 5117.
[12] (a) H.J. Batista, A.V.M. de Andrade, R.L. Longo, A.M. Simas, G.F. de Sa, N.K. Ito, L.C. Thompson, Inorg. Chem. 37 (1998) 3542;
(b) S.P.V. Nova, H.J. Batista, S. Alves Jr., C.M. Donega, R.L. Longo, G.F. de Sa, L.C. Thompson, J. Lumin. 118 (2006) 83.
[13] (a) P.C. Christidis, I.A. Tossidis, D.G. Paschalidis, L.C. Tzavellas, Acta Crystallogr. C54 (1998) 1233;
(b) M.O. Ahmed, J. Liao, X. Chen, S. Chen, J.H. Kaldis, Acta Crystallogr. E59 (2003) m29.
[14] Q. Zhong, H. Wang, G. Qian, Z. Wang, J. Zhang, J. Qiu, M. Wang, Inorg. Chem. 45 (2006) 4537.
[15] W.J. Evans, D.G. Giarikos, M.A. Johnston, M.A. Greci, J.W. Ziller, J. Chem. Soc., Dalton Trans. (2002) 520.
[16] A. Bellusci, G. Barberio, A. Crispini, M. Ghedini, M.L. Deda, D. Pucci, Inorg. Chem. 44 (2005) 1818.
[17] Z. Zheng, J. Wang, H. Liu, M.D. Carducci, N. Peyghambarian, G.E. Jabbourb, Acta Crystallogr. Sect. C58 (2002) m50.
[18] R. Wang, R. Wang, J. Yang, Z. Zheng, M.D. Carducci, T. Cayou, N. Peyghambarian, G.E. Jabbour, J. Am. Chem. Soc. 123 (2001) 6179.
[19] C.R. De Silva, J. Wang, M.D. Carducci, S.A. Rajapakshe, Z. Zheng, Inorg. Chim. Acta 357 (2004) 630.
[20] C.R. De Silva, R. Wang, Z. Zheng, Polyhedron 25 (2006) 3449.
[21] C.R. De Silva, J.R. Maeyer, A. Dawson, Z. Zheng, Polyhedron 26 (2007) 1229.
[22] A.A. Knyazev, V.S. Lobkov, Galyametdinov, G. Yu, Russian Chem. Bull. 53 (2004) 942.
[23] G. Barberio, A. Bellusci, A. Crispini, M. Ghedini, A. Golemme, P. Prus, D. Pucci, Eur. J. Inorg. Chem. (2005) 181.
[24] S.J.P. Bousquet, D.W. Bruce, J. Mater. Chem. 11 (2001) 1769.
[25] Bruker SAINT Reference Manual Version 5.0, Bruker AXS Inc., Madison, Wisconsin, USA, 1997.
[26] SADABS: Area-Detector Absorption Correction, Siemens Industrial Automation, Inc., Madison, WI, USA, 1996.
[27] F.R.G. Silva, O.L. Malta, C. Reinhard, H. Gudel, C. Piguet, J.E. Moser, J. Bünzli, J. Phys. Chem. A 106 (2002) 1670.
[28] R.F. Kubin, A.N. Fletcher, J. Lumin. 27 (1982) 455.
[29] (a) J.N. Demas, G.A. Crosby, J. Phys. Chem. 75 (1971) 991;
(b) J.V. Caspar, T.J. Meyer, J. Am. Chem. Soc. 105 (1983) 5583.
[30] (a) M. Shi, F. Li, T. Yi, D. Zhang, H. Hu, C. Huang, Inorg. Chem. 44 (2005) 8929;
(b) S. Quici, M. Cavazzini, G. Marzanni, G. Accorsi, N. Armaroli, B. Ventura, F. Barigelletti, Inorg. Chem. 44 (2005) 529.
[31] H. Bauer, J. Blanc, D.L. Ross, J. Am. Chem. Soc. 86 (1964) 5125.
[32] D.R. van Staverev, G.A. van Albada, J.G. Haasnoot, H. Kooijman, A.M.M. Lanfredi, P.J. Nieuwenhuizen, A.L. Spek, F. Ugozzoli, T. Weyhermuller, J. Reedijk, Inorg. Chim. Acta 315 (2001) 163.
[33] L. Thompson, J. Legendziewicz, J. Cybinska, L. Pan, W. Brennessel, J. Alloys Compd. 341 (2002) 312.
[34] A.Y. Rogachev, L.K. Minacheva, V.S. Sergienko, I.P. Malkerova, A.S. Alikhanyan, V.V. Stryapan, N.P. Kuzmina, Polyhedron 24 (2005) 723.
[35] R.C. Holz, L.C. Thompson, Inorg. Chem. 32 (1993) 5251.
[36] (a) M. Xiao, P.R. Selvin, J. Am. Chem. Soc. 123 (2001) 7067;
(b) S. Comby, D. Imbert, A. Chauvin, J.G. Bunzli, L.J. Charbonniere, R.F. Ziessel, Inorg. Chem. 43 (2004) 7369.
[37] M.H.V. Werts, R.T.F. Jukes, J.W. Verhoeven, Phys. Chem. Chem. Phys. 4 (2002) 1542.
[38] G.F. de Sa, O.L. Malta, C. de Mello Donega, A. M Simas, R.L. Longo, P.A. Santa-Cruz, E.F. da Silva Jr., Coord. Chem. Rev. 196 (2000) 165.